Published by Institute of Physics Publishing for SISSA/ISAS
Received: *January 7, 2005*
Accepted: *January 28, 2005*

One-loop MHV amplitudes in supersymmetric gauge theories

Callum Quigley[a] **and Moshe Rozali**[ab]

[a] *Department of Physics and Astronomy, University of British Columbia*
Vancouver, British Columbia V6T 1Z1, Canada
[b] *Kavli Institute for Theoretical Physics, University of California*
Santa Barbara, CA 93106-4030, U.S.A.
E-mail: cquigley@physics.ubc.ca, rozali@physics.ubc.ca

Abstract: Using CSW rules for constructing scalar Feynman diagrams from MHV vertices, we compute the contribution of $\mathcal{N} = 1$ chiral multiplet to one-loop MHV gluon amplitude. The result agrees with the one obtained previously using unitarity-based methods, thereby demonstrating the validity of the MHV-diagram technique, in the case of one-loop MHV amplitudes, for all massless supersymmetric theories.

Keywords: Gauge Symmetry, Hadronic Colliders.

JHEP01(2005)053

© SISSA/ISAS 2005

Contents

JHEP01(2005)053

1. Introduction and summary

Helicity amplitudes in gauge theories with massless matter exhibit remarkable simplicity, most manifest in the maximal helicity violating (MHV) amplitudes. For external gluons those are amplitudes with two negative helicity gluons and any number of positive helicity gluons (or vice versa). At tree level they are given by the Parke-Taylor formula, [1] which is holomorphic in the spinor variables characterizing the momenta of the external gluons. Such simplicity hints at a large symmetry structure which is hidden in the usual formulation of perturbation theory.

The simplification is not limited to MHV amplitude at tree level. In [2] a precise formulation[1] of the structure of helicity amplitudes was given: when transformed to twistor space, the helicity amplitudes are supported on certain algebraic curves. The precise type of algebraic curve depends on the detail of the amplitude, and grows more complicated with increasing number of loops or decreased helicity violation. The simplest such amplitudes are the Parke-Taylor ones, which are supported on lines in twistor space.

This structure led [4] to formulate effective Feynman rules for obtaining arbitrary helicity amplitudes using the Parke-Taylor amplitudes (continued to off-shell momenta) as vertices, combined with simple scalar propagators. We will call such Feynman graphs MHV-diagrams. Already in [4] a strong case was made that tree level helicity amplitudes are reproduced using these rules, and this was confirmed in a series of papers [5], for a review see [6]. Nevertheless a direct derivation of these rules from field theory is still lacking (see however [7]).

[1] See [3] for earlier related work.

The simple structure in twistor space motivates exploration of string theories with twistor target space [2, 8]. The original string theory in [2] indeed reproduces the tree level amplitudes [9] (the relation of these calculations to MHV-diagrams was explained in [10]). However the correspondence with the $\mathcal{N}=4$ amplitudes breaks down at one loop [11], due to non-decoupling of conformal supergravity modes.

The twistor space structure of one-loop diagrams was initially less clear, as they seem to be supported in twistor space on configurations different from one-loop MHV-diagrams [12]. Nevertheless, application of the MHV-diagram formalism in [13] reproduces the known result for one-loop MHV amplitude in $\mathcal{N}=4$ theory. The discrepancy was clarified by the existence of an holomorphic anomaly [14], which can be furthermore used to calculate unitarity cuts [15]. For further discussion of one-loop amplitudes in the $\mathcal{N}$=4 theory see [16].

So far all the one-loop results are restricted to the maximally supersymmetric case. As the formalism of MHV-diagrams lacks a field theory derivation, it is necessary to check it by reproducing the known one loop results, before using this efficient formalism to calculate unknown amplitudes. In this note we compute the contribution of the $\mathcal{N}=1$ chiral multiplet to the MHV one loop amplitudes. All MHV one-loop amplitudes in massless supersymmetric theory are a linear combination of this contribution, and that of a vector multiplet of $\mathcal{N}=4$ SYM, calculated in [13]. We therefore confirm that the MHV-diagram technique works for any supersymmetric theory at one-loop, at least for the amplitude we discuss. It seems that the success hinges more on the cut-constructibility [17], rather than supersymmetric cancelations. It would be interesting to check further whether this formalism is valid for non-supersymmetric (but still cut-constructible) cases.

This note is organized as follows: in section 2 we describe the CSW rules for constructing MHV diagrams [4], and their application to one-loop calculations in [13]. We also present the $\mathcal{N}=1$ amplitude constructed in [17], introducing our notations in the process. Section 3 includes our calculation, we follow closely the methods of [13]: we start by evaluating the MHV one-loop diagrams, we then arrange the result according to its cuts, and finally we perform the dispersion integration, which reproduces the amplitude from its cuts.

2. Background

2.1 One-loop MHV diagrams

The CSW rules [4] for constructing MHV diagrams consist of using the MHV amplitudes with two negative helicity gluons, as well as their supersymmetric partners, as the basic building blocks for obtaining all amplitudes (including the so-called googly ones, which have two positive helicity gluons, and therefore are also MHV).

Denote all incoming momenta into a vertex by k_i. The CSW prescription associates with each such momentum a spinor λ_i. For null momenta, $k_i^2=0$ the assignment follows from the decomposition $k_i^\mu = (\sigma^\mu)_{\alpha\dot\alpha}(\lambda_i)^\alpha(\bar\lambda_i)^{\dot\alpha}$. For general massive momenta this decomposition is impossible. Instead one chooses arbitrary spinors $\eta, \bar\eta$, equivalent to the choice

JHEP01(2005)053

of a lightcone frame, and decomposes each off-shell momentum k_i as

$$(k_i)^{\alpha\dot{\alpha}} = (\lambda_i)^{\alpha}(\bar{\lambda}_i)^{\dot{\alpha}} + z_i(\eta)^{\alpha}(\bar{\eta})^{\dot{\alpha}}\,. \tag{2.1}$$

The new variables z_i express how virtual are the momenta k_i.

Having chosen spinors λ_i for all momenta k_i, the vertices in the diagrams are the holomorphic Parke-Taylor amplitudes. When labeling all momenta cyclically, in clockwise direction, the purely gluonic vertices[2] are

$$\langle p\ q\rangle^4 \prod_{i=1}^{n} \frac{1}{\langle i, i+1\rangle}\,, \tag{2.2}$$

where n is the number of gluons in the vertex (which can be arbitrary), the negative helicity gluons are in positions p, q, and we use the notation $\langle i\ j\rangle \equiv \epsilon_{\alpha\beta}(\lambda_i)^{\alpha}(\lambda_j)^{\beta}$ for any pair of spinors. For later use we also define $[i\,j] =\equiv \epsilon_{\dot{\alpha}\dot{\beta}}(\bar{\lambda}_i)^{\dot{\alpha}}(\bar{\lambda}_j)^{\dot{\beta}}$ and $\langle\lambda\,|P\,|\,\bar{\eta}\,] = P_{\alpha\dot{\beta}}(\lambda)^{\alpha}(\bar{\eta})^{\dot{\beta}}$.

The MHV vertices are connected by simple scalar propagators, i/L^2, for any off-shell momentum L. As explained in [13], when combined with the integration over all off-shell momenta, the result is independent of the lightcone direction chosen, and can be decomposed as

$$\frac{d^4L}{L^2} = 2i\, d^4\ell\, \delta^{(+)}(\ell^2)\, \frac{dz}{z}\,, \tag{2.3}$$

where $\ell = \lambda\bar{\lambda}$ is the null momentum associated to L by the CSW prescription, and $\delta^{(+)}(\ell^2)$ is precisely the Lorenz invariant phase space measure appearing in the calculation of unitarity cuts. The decomposition is crucial to the results of [13] and will play the same role for us: the appearance of the Lorenz invariant phase space measure allows us to use unitarity-based methods [17]. The final integration over the z-variables is a dispersion integration which reconstructs the amplitude from its cuts.

2.2 The $\mathcal{N} = 1$ amplitude

The contribution of the $\mathcal{N} = 1$ chiral multiplet to one-loop MHV amplitude was calculated in [17] using unitarity-cut methods. We quote here the result we reproduce later using the MHV one-loop diagrams. Our notation here is fairly similar to [12], who analyzed the twistor space structure of this amplitude.

The result obtained in [17] is then:

$$\mathcal{A}_{\text{chiral}} = \frac{\mathcal{A}_{\text{tree}}}{32\pi^2}\left\{\sum_{r,s} b_{rs}^{pq} B(k_r, Q, k_s, P) + \sum_{r,s} c_{rs}^{pq} T(k_r, P, \widetilde{Q}) + \sum_{r,s} c_{sr}^{pq}\, T(k_s, Q, \widetilde{P}) + \mathcal{A}_{IR}\right\}, \tag{2.4}$$

where $\mathcal{A}_{tree}$ is the tree level MHV amplitude, and p, q are the locations of the negative helicity gluons. The first term in the parentheses comes from scalar (2-mass) box diagram, then there are two terms coming from scalar (two-mass) triangles and finally the last part $\mathcal{A}_{IR}$ comes from exceptional, boundary terms. The explicit form of the functions and some of their properties are summarized in [17, appendix II], and is also summarized below.

[2] We introduce the supersymmetric partners of these vertices in the next section.

JHEP01(2005)053

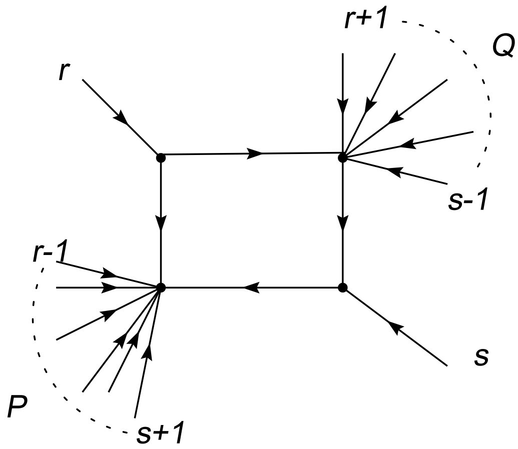

Figure 1: Diagrams contributing to box functions.

JHEP01(2005)053

We now explain our notation in formula (2.4), including the ranges of all summations. First, the box functions $B(k_r, Q, k_s, P)$ are the finite part of those appearing in the $\mathcal{N} = 4$ theory. Using the representation discovered in [13], they are

$$\begin{aligned} B(k_r, Q, k_s, P) &= F(k_r, Q, k_s, P) + \frac{1}{\epsilon^2}\left[(-s)^{-\epsilon} + (-t)^{-\epsilon} - (-P^2)^{-\epsilon} - (-Q^2)^{-\epsilon}\right] \\ &= \mathrm{Li}_2(1 - aP^2) + \mathrm{Li}_2(1 - aQ^2) - \mathrm{Li}_2(1 - as) - \mathrm{Li}_2(1 - at)^2\,, \end{aligned} \tag{2.5}$$

where we have introduced the momentum invariants $s = (P + k_r)^2$ and $t = (P + k_s)^2$ and the quantity a is defined

$$a = \frac{P^2 + Q^2 - s - t}{P^2 Q^2 - st}\,. \tag{2.6}$$

These functions are characterized by two massless external legs, with momenta k_r, k_s. The remaining momenta are then arranged uniquely into two massive external legs with momenta P, Q. The range of summation over r, s in (2.4) is restricted such that p belongs to the set of momenta in $P = k_{s+1} + \cdots + k_{r-1}$, and likewise q is one of the momenta in $Q = k_{r+1} + \ldots + k_{s-1}$. In particular the massless momenta k_r, k_s always have positive helicity. The set of diagrams contributing to the box functions is drawn in figure 1.

The triangle diagrams have similarly one massless momentum $k_{r,s}$, and two massive ones: $P, \widetilde{Q} \equiv Q + k_s$ or $Q, \widetilde{P} \equiv P + k_r$, each of which contains a single negative helicity gluon. Furthermore, to posses two massive legs requires $|r - s| > 1$ and $|r - s - 1| > 1$. The form of the two triangle functions are identical, in general

$$T(k, P, Q) = \frac{\log(P^2) - \log(Q^2)}{P^2 - Q^2}\,. \tag{2.7}$$

The two ranges of summations only differ from those of the box functions in that the first sum includes $s = q$ and the second $r = p$. Note also that the coefficients c_{rs}^{pq} depend on which leg is null, as explained below. The set of diagrams contributing to triangle functions $T(k_r, P, \widetilde{Q})$ is drawn in figure 2, the others follow the same pattern.

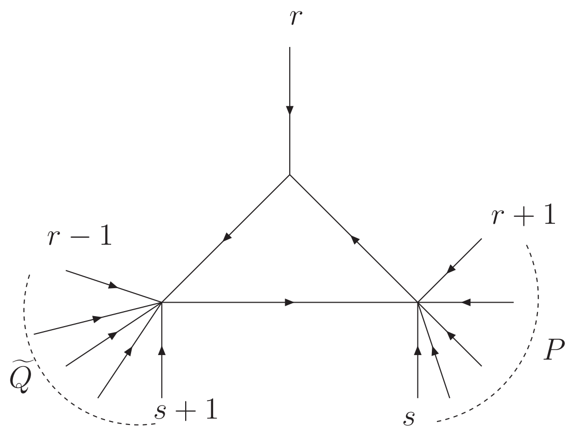

Figure 2: Diagrams contributing to triangle functions.

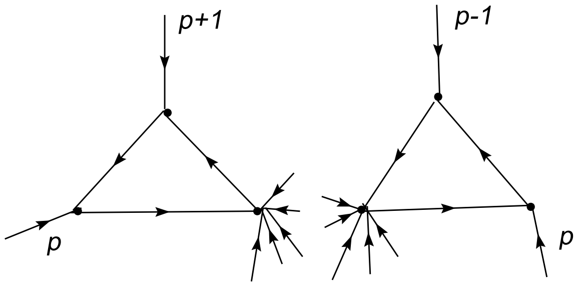

Figure 3: Two of the degenerate triangle diagrams, the other two are obtained by exchanging p and q .

The last term $\mathcal{A}_{IR}$ arises from degenerations of triangle diagrams for which one of the massive momenta become massless, that is it contains only a single external momentum which is then necessarily a negative helicity gluon. There are four such degenerations, for which $p = P, \widetilde{P}$ or $q = Q, \widetilde{Q}$. These cases are drawn in figure 3, they give rise to the following 4 terms:

$$\mathcal{A}_{IR} = c^{pq}_{p+1,p-1} \frac{\left(-(k_{p+1}+k_{p-1})^2\right)^{-1-\epsilon}}{\epsilon(1-2\epsilon)} + c^{pq}_{p-1,p} \frac{\left(-(k_{p-1}+k_p)^2\right)^{-1-\epsilon}}{\epsilon(1-2\epsilon)} + (p \leftrightarrow q)\,. \tag{2.8}$$

Finally, the coefficients appearing in (2.4) are as follows. For the box functions

$$b^{pq}_{rs} = 2\frac{\langle p\; r\rangle\langle p\; s\rangle\langle q\; r\rangle\langle q\; s\rangle}{\langle r\; s\rangle^2\langle p\, q\rangle^2} \tag{2.9}$$

whereas for the triangles (and the boundary terms) one has

$$c^{pq}_{rs} = \frac{\langle p\; r\rangle\langle r\; q\rangle}{\langle p\; q\rangle^2} \frac{\langle s, s+1\rangle}{\langle s\; r\rangle\langle s, r+1\rangle} \left(\langle q\; r\rangle\langle p\,|P\,|r] + \langle p\; r\rangle\langle q\,|P\,|r]\right). \tag{2.10}$$

Notice for c^{pq}_{sr} we must change $P = k_{s+1} + \cdots + k_{r-1}$ to $Q = k_{r+1} + \cdots + k_{s-1}$.

JHEP01(2005)053

3. The MHV diagram

3.1 Reduction of the diagram

We are interested in calculating the contribution of $N = 1$ chiral multiplet to one-loop MHV amplitudes. We consider the case of external gluons only, but many other diagrams with external fermions or scalar are related to this amplitude by supersymmetry. The one-loop diagram we compute is MHV, having two negative helicity gluons and arbitrary number of positive helicity ones.

The typical one loop MHV diagram of interest is drawn in figure 4. We must have one negative helicity gluon on each side of the diagram, as there is no possible helicity assignment for the intermediate states if both negative helicity gluons are on the same side of the diagram. We label the momenta on the left side as $k_{m_1}, \dots, k_{m_2}$, one of which is negative helicity, denoted by p. The momenta on the right side as $k_{m_2+1}, \dots, k_{m_1-1}$, the negative helicity momentum labeled q. All momentum labels are cyclically ordered. When calculating the complete amplitude one has to sum over such MHV diagram, we will arrange this sum according to the cuts, following [13]. All loop momenta are evaluated using dimensional regularization, in D dimensions, with $D = 4 - 2\epsilon$.

Now the amplitude for the diagram in figure 4 is given by

$$A^{1-\mathrm{loop}}_{\mathrm{chiral}} = i(2\pi)^4\delta(P_L + P_R)\int \frac{d^4L_1}{L_1^2}\int \frac{d^4L_2}{L_2^2}\delta^{(4)}(L_1 - L_2 + P_L)\left(A_L^F A_R^{\tilde{F}} + A_L^{\tilde{F}} A_R^F + 2A_L^S A_R^S\right), \tag{3.1}$$

where P_L, P_R are the momenta flowing into the diagrams from the left and right correspondingly. The factors A_L, A_R are related by supersymmetry to the gluonic MHV introduced above. Each vertex is obtained by combining the external gluons with two internal lines, which are members of a chiral multiplet, including a fermion (of two helicities, resulting in vertices A^F and $A^{\tilde{F}}$) and a complex scalar (resulting in a vertex A^S).

As reviewed above, each of the off-shell momenta $L_i, i = 1, 2$ can be associated a null momentum ℓ_i and the corresponding spinors $\ell_i = \lambda_i \bar{\lambda}_i$. These are necessary in order to write the off-shell vertices. We have therefore $L_i = \ell_i + z_i \eta\bar{\eta}$.

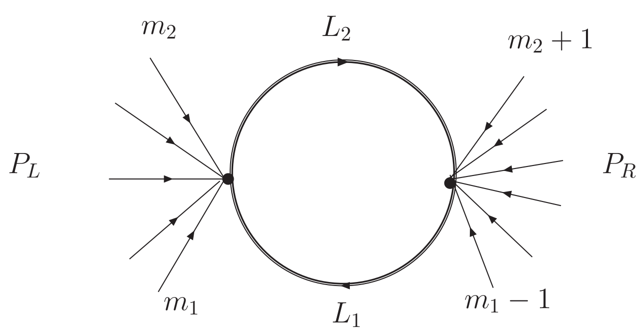

Figure 4: Typical one-loop MHV diagram, one has to sum over all choices of m_1, m_2. The negative helicity gluon p is on the left, and q is on the right.

JHEP01(2005)053

Factoring out the tree (Parke-Taylor) amplitude results[3] in:

$$A^{1-\text{loop}}_{\text{chiral}} = A_{\text{tree}} \int \frac{d^4L_1}{L_1^2} \int \frac{d^4L_2}{L_2^2} \delta^{(4)}(L_1 - L_2 + P_L) \frac{1}{\langle \lambda_1\ \lambda_2\rangle\langle \lambda_2\ \lambda_1\rangle} \left(2I^S + I^F + I^{\tilde{F}}\right) \times$$
$$\times \frac{\langle m_2\ m_2+1\rangle\langle m_1-1\ m_1\rangle}{\langle \lambda_1\ m_1\rangle\langle m_2\ \lambda_2\rangle\langle \lambda_2, m_2+1\rangle\langle m_1-1, \lambda_1\rangle}, \tag{3.2}$$

where

$$\begin{aligned} I^S &= \frac{\langle \lambda_1\ p\rangle^2\langle \lambda_2\ p\rangle^2\langle \lambda_1\ q\rangle^2\langle \lambda_2\ q\rangle^2}{\langle p\ q\rangle^4} \\ I^F &= -I^S \frac{\langle \lambda_2\ q\rangle\langle \lambda_1\ p\rangle}{\langle \lambda_2\ p\rangle\langle \lambda_1\ q\rangle} \\ I^{\tilde{F}} &= -I^S \frac{\langle \lambda_2\ p\rangle\langle \lambda_1\ q\rangle}{\langle \lambda_2\ p\rangle\langle \lambda_1\ q\rangle}\,. \end{aligned} \tag{3.3}$$

To sum the 3 terms in (3.2) one uses the Schouten identity

$$\langle a\ b\rangle\langle c\ d\rangle = \langle a\ d\rangle\langle c\ b\rangle + \langle a\ c\rangle\langle b\ d\rangle \tag{3.4}$$

which will be repeatedly used below. This leads to the following expression for the chiral multiplet contribution to the one loop gluon MHV amplitude

$$A^{1-\text{loop}}_{\text{chiral}} = A_{\text{tree}} \int \frac{d^4L_1}{L_1^2} \int \frac{d^4L_2}{L_2^2} \delta^{(4)}(L_1 - L_2 + P_L)\ R \tag{3.5}$$

with

$$R = \frac{\langle m_1-1, m_1\rangle\langle m_2, m_2+1\rangle\langle \lambda_1\ q\rangle\langle \lambda_2\ q\rangle\langle \lambda_1\ p\rangle\langle \lambda_2\ p\rangle}{\langle p\ q\rangle^2\langle m_1-1, \lambda_1\rangle\langle \lambda_1\ m_1\rangle\langle m_2\ \lambda_2\rangle\langle \lambda_2, m_2+1\rangle}\,. \tag{3.6}$$

Our next step is to split the spinor expression R into 4 terms of identical structure. Using the pair of Schouten identities:

$$\begin{aligned} \langle m_1-1, m_1\rangle\langle \lambda_1\ q\rangle &= \langle m_1-1, q\rangle\langle \lambda_1\ m_1\rangle + \langle m_1-1, \lambda_1\rangle\langle m_1\ q\rangle \\ \langle m_2, m_2+1\rangle\langle \lambda_2\ p\rangle &= \langle m_2\ p\rangle\langle \lambda_2, m_2+1\rangle + \langle m_2\ \lambda_2\rangle\langle m_2+1, p\rangle \end{aligned} \tag{3.7}$$

one gets the following sum:

$$R = R(m_2, m_1-1) - R(m_2+1, m_1-1) - R(m_2, m_1) + R(m_2+1, m_1) \tag{3.8}$$

where

$$R(r,s) = \frac{\langle \lambda_1\ p\rangle\langle \lambda_2\ q\rangle}{\langle p\ q\rangle^2} \frac{\langle s\ q\rangle\langle r\ p\rangle}{\langle s\ \lambda_1\rangle\langle r\ \lambda_2\rangle}\,. \tag{3.9}$$

Let us simplify $R(r,s)$: once again one uses Schouten identities to split $R(r,s)$ to 4 term, which (when integrated) give rise to tensor box, triangle and bubble diagrams. The

[3] We do not keep track of the overall sign, which can be fixed at the end of the calculation.

JHEP01(2005)053

4 terms are:

$$\begin{aligned}
R^A(r,s) &= \frac{\langle s\ q\rangle\langle r\ p\rangle\langle r\ q\rangle\langle ps\rangle}{\langle p\ q\rangle^2\langle r\ s\rangle^2}\frac{\langle\lambda_2\ s\rangle\langle\lambda_1\ r\rangle}{\langle\lambda_1\ s\rangle\langle\lambda_2\ r\rangle}\\
R^B(r,s) &= \frac{\langle s\ q\rangle\langle r\ p\rangle^2\langle r\ q\rangle}{\langle p\ q\rangle^2\langle r\ s\rangle^2}\frac{\langle\lambda_2\ s\rangle}{\langle\lambda_2\ r\rangle}\\
R^C(r,s) &= \frac{\langle s\ q\rangle^2\langle r\ p\rangle\langle s\ p\rangle}{\langle p\ q\rangle^2\langle r\ s\rangle^2}\frac{\langle\lambda_1\ r\rangle}{\langle\lambda_1\ s\rangle}\\
R^D(r,s) &= \frac{\langle s\ q\rangle^2\langle r\ p\rangle^2}{\langle p\ q\rangle^2\langle r\ s\rangle^2}\,.
\end{aligned} \tag{3.10}$$

Let us simplify these expressions one at a time:

- Simplifying R^A.

  We decompose the tensor box function R^A, as in [17, 13], into scalar components by expanding

$$\begin{aligned}
\frac{\langle s\ \lambda_2\rangle\langle r\ \lambda_1\rangle}{\langle r\ \lambda_2\rangle\langle s\ \lambda_1\rangle} &= \frac{[\lambda_2\ r]\langle r\ \lambda_1\rangle[\lambda_1\ s]\langle s\ \lambda_2\rangle}{\langle r\ \lambda_2\rangle[\lambda_2\ r]\langle s\ \lambda_1\rangle[\lambda_1\ s]} = -\frac{\mathrm{tr}(\frac{1}{2}(1-\gamma^5)\not\ell_2\not k_r\not\ell_1\not k_s)}{(\ell_2-k_r)^2(\ell_1+k_s)^2} = \\
&= \frac{-2\left\{(\ell_2\cdot k_r)(\ell_1\cdot k_s)+(\ell_2\cdot k_s)(\ell_1\cdot k_r)-(k_r\cdot k_s)(\ell_1\cdot\ell_2)+i\varepsilon_{\mu\nu\rho\sigma}\ell_2^\mu k_r^\nu\ell_1^\rho k_s^\sigma\right\}}{(\ell_2-k_r)^2(\ell_1+k_s)^2}\,.
\end{aligned} \tag{3.11}$$

  The term proportional to the ε-tensor vanishes upon integration. One can define $P_{L;z}=\ell_1-\ell_2=P_L-(z_1-z_2)\eta\bar\eta$, then the rest of the numerator may be rewritten as

$$\begin{aligned}
&\left(2(P_{L;z}\cdot k_r)(P_{L;z}\cdot k_s)-(k_r\cdot k_s)P_{L;z}^2\right)-(\ell_1+k_s)^2(P_{L;z}\cdot k_r)-\\
&-(\ell_2-k_r)^2(P_{L;z}\cdot k_s)+(\ell_2-k_r)^2(\ell_1+k_s)^2\,.
\end{aligned} \tag{3.12}$$

  The terms collected in the first brackets contribute to a scalar box integral, while the next two terms each contain a factor which cancels one of the propagators in the denominator , leaving scalar triangles. The last term reduces to a scalar bubble, since both propagators cancel. Next, we make use of the identity

$$4(P\cdot i)(P\cdot j)-2P^2(i\cdot j)=(P+i)^2(P+j)^2-P^2(P+i+j)^2\,, \tag{3.13}$$

  valid for any momentum P and null momenta i and j, to rewrite the box's coefficient in terms the shifted momentum invariants, defined as $s_z=(P_{L;z})^2, P_z^2=(P_{L;z}-k_r)^2, t_z=(P_{L;z}-k_r+k_s)^2$, and $Q_z^2=(P_{L;z}+k_s)^2$:

$$2(P_{L;z}\cdot k_r)(P_{L;z}\cdot k_s)-(k_r\cdot k_s)P_{L;z}^2=\frac{1}{2}(P_z^2Q_z^2-s_zt_z)\,. \tag{3.14}$$

  Thus, the result of the tensor box's decomposition is

$$\frac{\langle s\ \lambda_2\rangle\langle r\ \lambda_1\rangle}{\langle r\ \lambda_2\rangle\langle s\ \lambda_1\rangle}=\left\{\frac{\frac{1}{2}(P_z^2Q_z^2-s_zt_z)}{(\ell_2-k_r)^2(\ell_1+k_s)^2}-\frac{P_{L;z}\cdot k_r}{(\ell_2-k_r)^2}-\frac{P_{L;z}\cdot k_s}{(\ell_1+k_s)^2}\right\}+1\,. \tag{3.15}$$

JHEP01(2005)053

The terms collected in the bracket are the integrand of a (divergence free) scalar box function, complete with the correct coefficient b_{rs}^{pq}, as in equation (2.4). The second term contributes to scalar bubbles, which cancel against other contributions. We demonstrate this cancelation below.

- Simplifying R^B and R^C.

  We now turn to the linear triangle terms $R^B(r,s)$ and $R^C(r,s)$. First, we write the loop momentum dependant part of $R^B(r,s)$ as

$$\frac{\langle s\ \lambda_2\rangle}{\langle \lambda_2\ r\rangle} = -\frac{\langle s\ \lambda_2\rangle[\lambda_2\ r]}{\langle r\ \lambda_2\rangle[\lambda_2\ r]} = \frac{\langle s|\ell_2|r]}{(\ell_2-k_r)^2} = \langle s|\gamma_\mu|r]\frac{\ell_2^\mu}{(\ell_2-k_r)^2}\,. \tag{3.16}$$

So, R^B is the integrand of the (cut) linear two-mass triangle integral $I^{2m}_{3:r-m_1;m_1}[\ell_2^\mu]$, defined in [17]. Next, we use the decomposition of the linear triangle given in [17]:

$$I^{2m}_{3:r;i}[k^\mu] = -(P_z+k_r)^\mu I^{2m}_{3:r;i}[y] - k_r^\mu I^{2m}_{3:r;i}[z]\,, \tag{3.17}$$

where the arguments in square brackets are the numerators in the integrals, y and z are Feynmann parameters, P_z is the momentum of one massive leg (shifted by z dependent terms, as defined above) and k_r is the momentum of the massless leg, as drawn in figure 3. Since $[r\ r]=0$, we can write

$$\langle s|\gamma_\mu|r]I^{2m}_{3:r-m_1;m_1}[\ell_2^\mu] = -\langle s|P_z|r]I^{2m}_{3:r-m_1;m_1}[y]\,. \tag{3.18}$$

Now, the full coefficient of R^B is

$$-\frac{\langle p\ r\rangle\langle r\ q\rangle\langle p\ r\rangle\langle s\ q\rangle\langle s\ P_z\rangle[P_z\ r]}{\langle p\ q\rangle^2\langle r\ s\rangle^2}\,. \tag{3.19}$$

Applying the Schouten identity to the terms $\langle p\ r\rangle\langle s\ P_z\rangle$ and $\langle r\ q\rangle\langle s\ P_z\rangle$, then averaging over the two gives

$$\begin{aligned}&-\frac{\langle p\ r\rangle\langle s\ q\rangle}{\langle p\ q\rangle^2\langle r\ s\rangle}\left(\frac{\langle p\ r\rangle\langle q\ P_z\rangle+\langle q\ r\rangle\langle p\ P_z\rangle}{2}\right)[P_z\ r]-\\ &-\frac{\langle p\ r\rangle\langle s\ q\rangle}{\langle p\ q\rangle^2\langle r\ s\rangle^2}\left(\frac{\langle p\ s\rangle\langle r\ q\rangle+\langle p\ r\rangle\langle s\ q\rangle}{2}\right)2(P_z\cdot k_r)\,.\end{aligned} \tag{3.20}$$

We use the Schouten identity again, on the first term of the first pair only.

$$\frac{\langle p\ r\rangle\langle s\ q\rangle}{\langle r\ s\rangle} = \frac{\langle p\ s\rangle\langle r\ q\rangle}{\langle r\ s\rangle}+\langle p\ q\rangle\,. \tag{3.21}$$

Note that the piece containing $\langle p\ q\rangle$ is independent of s, so it will vanish when summing over $s=\{m_1-1,m_1\}$, as that sum has alternating signs. Now the first pair of terms in equation (3.20) reads

$$\frac{\langle p\ r\rangle\langle r\ q\rangle}{\langle r\ s\rangle\langle p\ q\rangle^2}\left(\frac{\langle s\ q\rangle\langle p\ P_z\rangle+\langle s\ p\rangle\langle q\ P_z\rangle}{2}\right)[P_z\ r]\,. \tag{3.22}$$

JHEP01(2005)053

A similar analysis of $R^C(r,s)$ shows that the coefficient of the integral function $I^{2m}_{3:s-m_2+1;m_2+1}[y]$ is

$$\frac{\langle p\ s\rangle\langle s\ q\rangle}{\langle r\ s\rangle\langle p\ q\rangle^2}\left(\frac{\langle r\ p\rangle\langle q\ Q_z\rangle+\langle r\ q\rangle\langle p\ Q_z\rangle}{2}\right)[Q_z\ s]+ \\ +\frac{\langle p\ r\rangle\langle s\ q\rangle}{\langle r\ s\rangle^2\langle p\ q\rangle^2}\left(\frac{\langle p\ s\rangle\langle r\ q\rangle+\langle p\ r\rangle\langle s\ q\rangle}{2}\right)2(Q_z\cdot k_s)\,, \tag{3.23}$$

where Q_z is the shifted momentum transfer defined above. In this decomposition the first term contributes to the coefficient of the scalar triangle function, and the second one will be used below to cancel the bubble diagrams.

- Simplifying R^D.

  First,the scalar bubble in R^D can be combined with that discussed above, in R^A, giving a single bubble with coefficient

$$\frac{\langle p\ r\rangle\langle s\ q\rangle}{\langle r\ s\rangle\langle p\ q\rangle^2}\left(\langle p\ s\rangle\langle r\ q\rangle+\langle p\ r\rangle\langle s\ q\rangle\right). \tag{3.24}$$

  Now, to cancel the bubbles notice that they posses the same coefficient as the last pair of terms in equations. (3.20) and (3.23). These integrals combine into

$$\frac{\langle p\ r\rangle\langle s\ q\rangle}{\langle r\ s\rangle^2\langle p\ q\rangle^2}\left(\frac{\langle p\ s\rangle\langle r\ q\rangle+\langle p\ r\rangle\langle s\ q\rangle}{2}\right)\circ \\ \circ\left(2I_{2:r-m_1;m_1}-2(P_z\cdot k_r)I^{2m}_{3:r-m_1;m_1}[y]+2(Q_z\cdot k_s)I^{2m}_{3:s-m_2+1;m_2+1}[y]\right), \tag{3.25}$$

  which vanishes in each channel of each cut because of the relation

$$(t_i^{[r+1]}-t_i^{[r]})I^{2m}_{3:r;i}[y]=I_{2:r;i}-I_{2:r+1;i}\,. \tag{3.26}$$

  Here we have introduced the additional notation $t_i^{[r]}=(k_i+k_{i+1}+\cdots+k_{i+r-1})^2$.

In summary, the net result of this decomposition is then

$$R(r,s) = \frac{\langle p\ r\rangle\langle r\ q\rangle\langle p\ s\rangle\langle s\ q\rangle}{\langle r\ s\rangle^2\langle p\ q\rangle^2}\left\{\frac{\frac{1}{2}(P_z^2Q_z^2-s_zt_z)}{(\ell_2-k_r)^2(\ell_1+k_s)^2}-\frac{P_{L;z}\cdot k_r}{(\ell_2-k_r)^2}-\frac{P_{L;z}\cdot k_s}{(\ell_1+k_s)^2}\right\}+ \\ +\frac{\langle p\ r\rangle\langle r\ q\rangle}{\langle r\ s\rangle\langle p\ q\rangle^2}\left\{\frac{\langle s\ q\rangle\langle p|P_z|r]+\langle s\ p\rangle\langle q|P_z|r]}{2}\right\}\frac{\left(\frac{\epsilon}{1-2\epsilon}\right)}{(\ell_2-k_r)^2}+ \\ +\frac{\langle p\ s\rangle\langle s\ q\rangle}{\langle r\ s\rangle\langle p\ q\rangle^2}\left\{\frac{\langle r\ p\rangle\langle q|Q_z|s]+\langle r\ q\rangle\langle p|Q_z|s]}{2}\right\}\frac{\left(\frac{\epsilon}{1-2\epsilon}\right)}{(\ell_1+k_s)^2}\,, \tag{3.27}$$

where we have used the fact that

$$I^{2m}_{3:r;i}[y]=\frac{\epsilon}{1-2\epsilon}I^{2m}_{3:r;i}[1] \tag{3.28}$$

to conveniently express the triangles' integrands.

JHEP01(2005)053

The first coefficient above is easily recognizable as $\frac{1}{2}b_{rs}^{pq}$ from equation (2.9), but to get the remaining two into the correct form requires an additional step. Consider the second line of each of the four $R(r,s)$ terms. Those with a common value for r differ only in the s dependance of their coefficients. So when we add $R(r,m_1-1)-R(r,m_1)$, the only change is

$$\sum_s \frac{\langle s\ x\rangle}{\langle r\ s\rangle} = \frac{\langle m_1-1\ x\rangle}{\langle r\ m_1-1\rangle} - \frac{\langle m_1\ x\rangle}{\langle r\ m_1\rangle} = \frac{\langle x\ r\rangle\langle m_1-1\ m_1\rangle}{\langle m_1-1\ r\rangle\langle r\ m_1\rangle}\,, \tag{3.29}$$

where $x=p,q$, and we used the Schouten identity to combine the two terms. Now the coefficient of the second line is $\frac{1}{2}c_{r(m_1-1)}^{pq}$. An analogous treatment of the third line produces the coefficient $\frac{1}{2}c_{sm_2}^{pq}$.

3.2 Combinatorics of cuts

We have decomposed the integrand of each one of the MHV diagrams into a sum (3.27) which should now be compared with the sum occurring in the exact result (2.4). The crucial point is the decomposition of the measure [13]:

$$\frac{d^4L_1}{L_1^2}\frac{d^4L_1}{L_1^2}\delta^{(4)}(L_1-L_2+P_L) = -4\frac{dz_1}{z_1}\frac{dz_2}{z_2}\,dLIPS(\ell_2,-\ell_1,P_{L,z})\,, \tag{3.30}$$

where dLIPS is the Lorenz invariant phase space measure appearing in the cut rules. For fixed z_1,z_2 we have then, after performing the integration over l_1,l_2 sum over cuts of Feynman graphs (at shifted values of the momentum invariant). The claim is that this sum, at $z=0$, coincides exactly with the cut of the exact result (2.4). This is not true diagram by diagram, rather there is some re-arrangement of the cuts which we now demonstrate.

Having completed the decomposition of $R=\sum_{r,s}R(r,s)$ in the previous section, we find it contains eight distinct terms which are: 4 (cut) two-mass finite box functions (1 for each pair of null legs k_r and k_s), and 4 modified (cut) two-mass triangles (1 for each case where k_r or k_s is the null leg). When we cut the loop in the MHV diagram, this is equivalent to cutting the boxes and triangles, as shown in figure 5, so as to keep $\{k_{m_1},\ldots,k_{m_2}\}$ on the same side of the cut. Clearly, which lines get cut depends completely on where k_{m_1},k_{m_2} are in relation to k_r,k_s. We stress that all these cuts are in the same channel, s. Alternatively, we could combine the contributions from different MHV diagrams (with different m_1,m_2) which have the same null legs k_r,k_s and therefore must produce the same boxes and triangles. Different MHV diagrams will lead to different cuts. In this manner, we may combine: the 4 boxes with common k_r and k_s, with cuts in the channels s,t,P^2,Q^2, the 2 triangles with common k_r, with cuts in the channels $s=\widetilde{Q}^2$ and P^2, and the 2 triangles with common k_s, with cuts in the channels $s=\widetilde{P}^2$ and Q^2, for all values of r,s.

In the exceptional cases where one of the triangles massive legs becomes massless, then this diagram has the single non-trivial cut which isolates the remaining massive leg. We will show below that each of these terms are reconstructed from their single cut.

One might worry that not all the cuts exist in all channels for non-degenerate cases. A priori, we must sum over all MHV diagrams with $q+1\leq m_1\leq p$ and $p\leq m_2\leq q-1$, but when $m_2=p$ or $m_1-1=q$ the corresponding boxes and triangles may not be defined.

JHEP01(2005)053

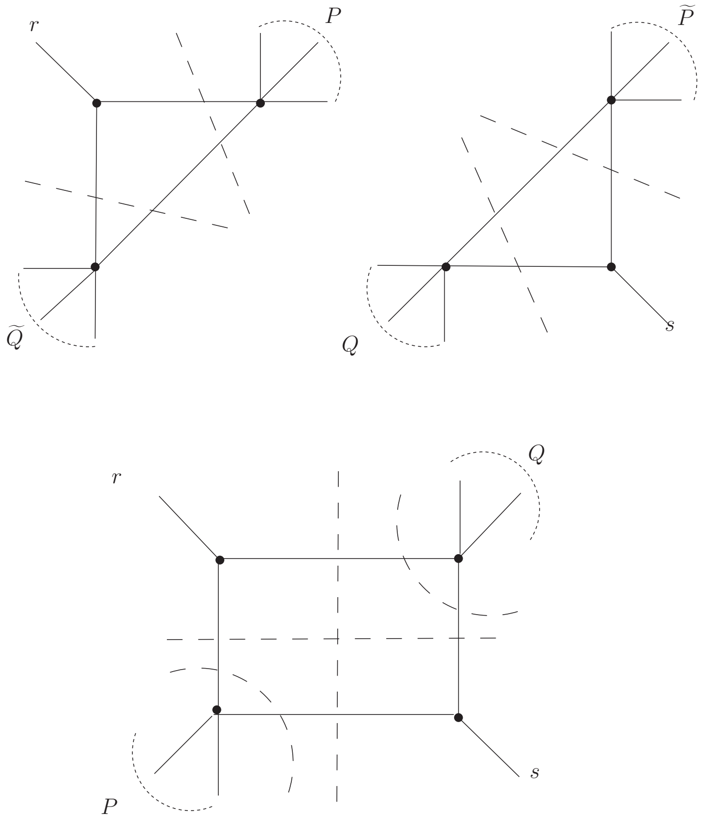

Figure 5: One MHV diagram produces 4 cut boxes and triangles, one for each dashed line. Where exactly the cut lies depends on r, s. Therefore, a given box (triangle) with r, s fixed requires 4 (2) MHV diagrams to produce all of its cuts.

Fortunately, the coefficients

$$b^{pq}_{ps} = b^{pq}_{rq} = c^{pq}_{ps} = c^{pq}_{qr} = 0 \tag{3.31}$$

all vanish. So, we may restrict the sums over $m_2 \equiv r, m_1 \equiv s+1$ to the ranges given in section 2.2, plus the degenerate triangle terms.

So, in summary, we have found that the decomposition of the sum of MHV diagram is simply related to the result (2.4). For any channel $X = s, t, P^2, Q^2$, of any function $F = B, T, \mathcal{A}_{IR}$ in (2.4), we find a term in our sum of the form $\Delta_X F(X_z)$, where Δ_X denotes the cut in the X-channel, and X_z is X shifted by z-dependent terms.

3.3 Calculating the cuts

In the last section, we noted that the loop integrations factor into two parts: dispersion integrals over the z_i and an integral over dLIPS$(\ell_2, -\ell_1, P_{L;z})$ which computes the cuts in the diagrams. The cut box integrals were computed in [13], so the only new ingredients are the cut triangles. We will now evaluate these integrals for when k_r is the null leg, the other case follows by switching $r \leftrightarrow s$ and $\ell_2 \leftrightarrow -\ell_1$. Also, we focus on the s-channel cuts; other channels are treated analogously. The integrals we wish to solve are in dimension

JHEP01(2005)053

$D = 4 - 2\epsilon$ and of the form

$$\mathcal{I}(s_z) = \int d^D\mathrm{LIPS}(\ell_2, -\ell_1, P_{L;z}) \frac{N(P_{L;z})}{(\ell_2 - k_r)^2}\,, \tag{3.32}$$

where the numerator $N(P_{L;z})$ only depends on $P_{L;z}$ and external momenta.[4] By boosting to the rest frame of $\ell_1 - \ell_2$, then rotating k_r into the x_D direction, we have

$$\ell_1 = \frac{1}{2}\,|P_{L;z}|\,(1, \mathbf{v})\,; \qquad \ell_2 = \frac{1}{2}\,|P_{L;z}|\,(-1, \mathbf{v})\,; \qquad k_r = (k_r, 0, \ldots, 0, k_r)\,, \tag{3.33}$$

where the unit vector $\mathbf{v}$ is such that $\mathbf{v} \cdot \widehat{x}_D = \cos(\theta_1)$. This allows us to re-write our phase-space measure as in [13]

$$d^D\mathrm{LIPS}(\ell_2, -\ell_1, P_{L;z}) = \frac{\pi^{\frac{1}{2}-\epsilon}}{4\Gamma(\frac{1}{2}-\epsilon)} \left|\frac{P_{L;z}^2}{4}\right|^{-\epsilon} d\theta_1 d\theta_2 (\sin\theta_1)^{1-2\epsilon}(\sin\theta_2)^{-2\epsilon} \tag{3.34}$$

and the integrand's denominator becomes

$$(\ell_2 - k_r)^2 = -2\ell_2 \cdot k_r = k_r\,|P_{L;z}|\,(1 - \cos\theta_1)\,. \tag{3.35}$$

Performing the integral (3.32) is now a simple task, with the result

$$\begin{aligned} \mathcal{I}(s_z) &= \frac{4^\epsilon \pi^{\frac{3}{2}-\epsilon}}{2\Gamma(\frac{1}{2}-\epsilon)} \left|\frac{s_z}{4}\right|^{-\epsilon} \frac{N(P_{L;z})}{k_r|P_{L;z}|} \frac{\Gamma(-\epsilon)}{\Gamma(1-\epsilon)} \\ &\to -\frac{1}{\epsilon}\frac{\pi}{2}\frac{N(P_{L;z})}{k_r|P_{L;z}|}\, s_z^{-\epsilon}\,. \end{aligned} \tag{3.36}$$

Now, for any channel of any function $F(X)$ appearing in the result (2.4), we are left with an integral of the form $\int \frac{dz_1}{z_1}\frac{dz_2}{z_2} \Delta_X F(X_z)$, where the cuts of the triangle graphs are exhibited in (3.36). Furthermore, we have shown that $\Delta_X F(X_{z=0})$ is precisely the cut of the exact result (2.4). Appealing to cut constructibility, we can anticipate that our dispersion integration will reproduce the correct answer as long as the functions $\Delta_X F(X_z)$ are cut free on the integration contour of the z-integration. As the cuts (3.36) do include non-analytic functions of X_z, the correct contour[5] is $X_z \geq 0$. Choosing such contour, it is a simple matter to perform the dispersion integration directly to verify that we get the correct answer, and we turn to that integration now.

3.4 Dispersion integrals

We now show that the final integrations over z_1, z_2 reproduce the result in (2.4). Recall that in section 3.2, we demonstrated that the sum over MHV diagrams is equivalent to the sum of cuts in all possible channels of the box and triangle diagrams. Thus, it remains to show that a given box (triangle) is reconstructed from the sum of its 4 (2) integrated cuts.

[4] Since [r r]=0, we can always write $\langle x|P_z|r] = \langle x|(P_z + k_r)|r] = \langle x|P_{L;z}|r]$, where $x = p, q$.

[5] We note that the integration contour then is channel-dependent, as in [13].

JHEP01(2005)053

We change our integration variables to $z \equiv z_1 - z_2$, $z' \equiv z_1 + z_2$ and note that for any function $f(z)$ independent of z'

$$\int \frac{dz_1}{z_1}\frac{dz_2}{z_2} f(z_1 - z_2) = 2(2\pi i)\int \frac{dz}{z} f(z)\,. \tag{3.37}$$

Next, we use the fact that $s_z = s - 2z\eta \cdot P_L$ to write

$$\frac{dz}{z} = -\frac{ds_z}{s - s_z}\,, \tag{3.38}$$

with a corresponding change of variables in the other channels. Now, we must show that

$$\begin{aligned} B(k_r, Q, k_s, P) = & \int \frac{ds_z}{s - s_z}\Delta_s B(s_z) + \int \frac{dt_z}{t - t_z}\Delta_t B(t_z) - \\ & - \int \frac{dP_z^2}{P^2 - P_z^2}\Delta_{P^2} B(P_z^2) - \int \frac{dQ_z^2}{Q^2 - Q_z^2}\Delta_{Q^2} B(Q_z^2) \end{aligned} \tag{3.39}$$

and

$$T(k, P, Q) = \int \frac{dP_z^2}{P^2 - P_z^2}\Delta_{P^2} T(P_z^2) - \int \frac{dQ_z^2}{Q^2 - Q_z^2}\Delta_{Q^2} T(Q_z^2)\,. \tag{3.40}$$

Again, we will consider the s-channel only, the other channels follow immediately. As discussed above, we must choose integration contour for which the integrands are analytic as functions of the kinematical variables. Therefore we restrict the integration to $s_z > 0$, where the expression (3.36) has no cuts.

First, we will reconstruct the divergence free box functions. They posses three types of terms, given in the first line of (3.27). The first of these was calculated in [13], we quote their result:

$$d^D\text{LIPS}\int \frac{ds_z}{s - s_z}\frac{\frac{1}{2}(Q_z^2 P_z^2 - s_z t_z)}{(\ell_2 - k_r)^2(\ell_1 - k_s)^2} = -\frac{1}{\epsilon^2}(-s)^{-\epsilon} - \text{Li}_2(1 - a\, s)\,. \tag{3.41}$$

The next term has the cut $\mathcal{I}(s_z)$ found earlier, with numerator $N(P_{L;z}) = -P_{L;z}\cdot k_r$. Up to a sign, this numerator is precisely the denominator in our working reference frame (3.33). The dispersion integral is then

$$-\frac{1}{2\epsilon}\int_0^\infty \frac{ds_z}{s - s_z}s_z^{-\epsilon} = \frac{1}{2}\frac{\pi\,\csc(\pi\epsilon)}{\epsilon}(-s)^{-\epsilon} \longrightarrow \frac{1}{2\epsilon^2}(-s)^{-\epsilon}\,. \tag{3.42}$$

The next term in the divergence free box gives an identical contribution. Summing the three contributions, we find

$$\int \frac{ds_z}{s - s_z}\Delta_s B(s_z) = -\text{Li}_2(1 - a\, s)\,, \tag{3.43}$$

exactly what is required to reproduce (2.5). Treating the other channels similarly proves the equality of (3.39) and (2.5).

Moving on to the triangles, we will consider those where k_r is the null leg. These also have cuts of the form $\mathcal{I}(s_z)$, in the reference frame (3.33) the numerator is

$$N(P_{L;z}) = \langle x|P_z|r] = \langle x|P_{L;z}|r] = \langle x|\gamma^0|r]\,|P_{L;z}| \tag{3.44}$$

JHEP01(2005)053

times $(\frac{\epsilon}{1-2\epsilon})$ and $x = p, q$. The dispersion integral is nearly identical to (3.42):

$$\frac{1}{2\epsilon}\int_0^\infty \frac{ds_z}{s-s_z}\frac{\epsilon}{1-2\epsilon}\frac{\langle x|\gamma^0|r]}{k_r}s_z^{-\epsilon} = \frac{1}{\epsilon(1-2\epsilon)}\frac{\langle x|\gamma^0|r]}{2k_r}(-s)^{-\epsilon}\,. \tag{3.45}$$

Multiplying the top and bottom by $|P| \equiv P^0$, then re-expressing this result in a covariant fashion gives the coefficient

$$\frac{\langle x|\gamma^0|r]}{2k_r} = \frac{\langle x|P|r]}{2k_r \cdot P} = \frac{\langle x|P|r]}{\widetilde{Q}^2 - P^2} \tag{3.46}$$

(recall that $s \equiv \widetilde{Q}^2$). An analogous result holds in the P^2 channel. Taking the difference of the two, and expanding $(-\widetilde{Q}^2)^{-\epsilon}, (-P^2)^{-\epsilon}$ in ϵ yeilds the desired result:

$$\frac{1}{\epsilon(1-2\epsilon)}\frac{(-\widetilde{Q}^2)^{-\epsilon} - (-P^2)^{-\epsilon}}{\widetilde{Q}^2 - P^2} = \frac{\log(\widetilde{Q}^2) - \log(P^2)}{\widetilde{Q}^2 - P^2}\,. \tag{3.47}$$

In the case of the one-mass triangles, the result is even simpler. Consider the case $(r, s) = (p+1, p-1)$, then $P^2 = p^2 = 0$ and the dispersion integral gives

$$\frac{1}{\epsilon(1-2\epsilon)}\frac{(-\widetilde{Q}^2)^{-\epsilon}}{\widetilde{Q}^2} \tag{3.48}$$

as desired. We conclude therefore that all triangle terms are reconstructed once we perform the final dispersion integration.

Thus, we have shown by explicit calculation that the MHV diagrams formalism is valid for the calculation of one-loop contribution of the $\mathcal{N} = 1$ chiral multiplet to the MHV amplitude. Together with the result of [13] this establishes the validity of the MHV-diagram technique for that amplitude in any massless supersymmetric theory. It would be interesting to check the formalism further by applying it to non-supersymmetric, but cut-constructible amplitudes.

Acknowledgments

We thank Zvi Bern for a useful comment. M.R. thanks the physics departments at Cornell and Syracuse, and the KITP at Santa Barbara for hospitality during the completion of this work. We are supported by National Science and Engineering Research Council of Canada. This research was supported in part by the National Science Foundation under Grant No. PHY99-0794

References

[1] S.J. Parke and T.R. Taylor, *An amplitude for N gluon scattering*, *Phys. Rev. Lett.* **56** (1986) 2459.

[2] E. Witten, *Perturbative gauge theory as a string theory in twistor space*, *Commun. Math. Phys.* **252** (2004) 189 [hep-th/0312171].

JHEP01(2005)053

[3] V.P. Nair, *A current algebra for some gauge theory amplitudes*, *Phys. Lett.* **B 214** (1988) 215.

[4] F. Cachazo, P. Svrcek and E. Witten, *MHV vertices and tree amplitudes in gauge theory*, *J. High Energy Phys.* **09** (2004) 006 [hep-th/0403047].

[5] C.J. Zhu, *The googly amplitudes in gauge theory*, *J. High Energy Phys.* **04** (2004) 032 [hep-th/0403115];
G. Georgiou and V.V. Khoze, *Tree amplitudes in gauge theory as scalar mhv diagrams*, *J. High Energy Phys.* **05** (2004) 070 [hep-th/0404072];
G. Georgiou, E.W.N. Glover and V.V. Khoze, *Non-MHV tree amplitudes in gauge theory*, *J. High Energy Phys.* **07** (2004) 048 [hep-th/0407027];
J.B. Wu and C.J. Zhu, *Mhv vertices and scattering amplitudes in gauge theory*, *J. High Energy Phys.* **07** (2004) 032 [hep-th/0406085]; *MHV vertices and fermionic scattering amplitudes in gauge theory with quarks and gluinos*, *J. High Energy Phys.* **09** (2004) 063 [hep-th/0406146];
D.A. Kosower, *Next-to-maximal helicity violating amplitudes in gauge theory*, hep-th/0406175;
X. Su and J.B. Wu, *Six-quark amplitudes from fermionic MHV vertices*, hep-th/0409228.

[6] V.V. Khoze, *Gauge theory amplitudes, scalar graphs and twistor space*, hep-th/0408233.

[7] Y. Abe, V.P. Nair and M.I. Park, *Multigluon amplitudes, $N = 4$ constraints and the WZW model*, *Phys. Rev.* **D 71** (2005) 025002 [hep-th/0408191].

[8] N. Berkovits, *An alternative string theory in twistor space for $N = 4$ super- Yang-Mills*, *Phys. Rev. Lett.* **93** (2004) 011601 [hep-th/0402045];
A. Neitzke and C. Vafa, *$N = 2$ strings and the twistorial Calabi-Yau*, hep-th/0402128;
N. Berkovits and L. Motl, *Cubic twistorial string field theory*, *J. High Energy Phys.* **04** (2004) 056 [hep-th/0403187];
W. Siegel, *Untwisting the twistor superstring*, hep-th/0404255.

[9] R. Roiban, M. Spradlin and A. Volovich, *A googly amplitude from the B-model in twistor space*, *J. High Energy Phys.* **04** (2004) 012 [hep-th/0402016];
R. Roiban and A. Volovich, *All conjugate-maximal-helicity-violating amplitudes from topological open string theory in twistor space*, *Phys. Rev. Lett.* **93** (2004) 131602 [hep-th/0402121];
R. Roiban, M. Spradlin and A. Volovich, *On the tree-level s-matrix of Yang-Mills theory*, *Phys. Rev.* **D 70** (2004) 026009 [hep-th/0403190].

[10] S. Gukov, L. Motl and A. Neitzke, *Equivalence of twistor prescriptions for super Yang-Mills*, hep-th/0404085;
I. Bena, Z. Bern and D.A. Kosower, *Twistor-space recursive formulation of gauge theory amplitudes*, hep-th/0406133.

[11] N. Berkovits and E. Witten, *Conformal supergravity in twistor-string theory*, *J. High Energy Phys.* **08** (2004) 009 [hep-th/0406051].

[12] F. Cachazo, P. Svrcek and E. Witten, *Twistor space structure of one-loop amplitudes in gauge theory*, *J. High Energy Phys.* **10** (2004) 074 [hep-th/0406177].

[13] A. Brandhuber, B. Spence and G. Travaglini, *One-loop gauge theory amplitudes in $N = 4$ super Yang-Mills from MHV vertices*, *Nucl. Phys.* **B 706** (2005) 150 [hep-th/0407214].

JHEP01(2005)053

[14] F. Cachazo, P. Svrcek and E. Witten, *Gauge theory amplitudes in twistor space and holomorphic anomaly*, *J. High Energy Phys.* **10** (2004) 077 [hep-th/0409245];
I. Bena, Z. Bern, D.A. Kosower and R. Roiban, *Loops in twistor space*, hep-th/0410054.

[15] F. Cachazo, *Holomorphic anomaly of unitarity cuts and one-loop gauge theory amplitudes*, hep-th/0410077;
R. Britto, F. Cachazo and B. Feng, *Computing one-loop amplitudes from the holomorphic anomaly of unitarity cuts*, hep-th/0410179.

[16] M.X. Luo and C.K. Wen, *One-loop maximal helicity violating amplitudes in $N = 4$ super Yang-Mills theories*, *J. High Energy Phys.* **11** (2004) 004 [hep-th/0410045];
M.X. Luo and C.K. Wen, *Systematics of one-loop scattering amplitudes in $N = 4$ super Yang-Mills theories*, hep-th/0410118;
Z. Bern, V. Del Duca, L.J. Dixon and D.A. Kosower, *All non-maximally-helicity-violating one-loop seven-gluon amplitudes in $N = 4$ super- Yang-Mills theory*, hep-th/0410224.

[17] Z. Bern, L.J. Dixon, D.C. Dunbar and D.A. Kosower, *Fusing gauge theory tree amplitudes into loop amplitudes*, *Nucl. Phys.* **B 435** (1995) 59 [hep-ph/9409265].

[18] W. Beenakker, H. Kuijf, W.L. van Neerven and J. Smith, *QCD corrections to heavy quark production in $p\bar{p}$ collisions*, *Phys. Rev.* **D 40** (1989) 54.

JHEP01(2005)053